Aggregation State of Spin-Labeled Cecropin AD in Solution†

Hassane S. Mchaourab, James S. Hyde,* and Jimmy B. Feix

Biophysics Research Institute, Medical College of Wisconsin, Milwaukee, Wisconsin 53226

Received June 28, 1993; Revised Manuscript Received August 24, 1993®

ABSTRACT: A spin-labeled derivative of the ion channel peptide cecropin AD (Fink *et al.*, 1988) was synthesized and used to investigate its aggregation state in water and in the presence of a helix-promoting solvent. A cysteine was introduced at position 33 and spin-labeled using the methanethiosulfonate spin label. In low ionic strength aqueous solution, the peptide is monomeric, and the ESR spectrum indicates a high degree of segmental flexibility at the nitroxide attachment point, consistent with a predominantly random coil conformation. Upon addition of 5–10% (v/v) hexafluoro-2-propanol (HFP), the peptide is induced to aggregate as evidenced by significant motional restriction of the spin label and spin–spin broadening of the ESR lines. At higher concentrations of HFP, the peptide reverts to a monomeric state but retains its folded conformation. Our data suggest that between 5 and 10% HFP the peptide undergoes two structural transitions. The first transition starts at 5% and is very cooperative. Its dependence on ionic strength, temperature, and pH indicates that it involves the interconversion between a random coil and an ordered state stabilized by interpeptide electrostatic and hydrophobic interactions. The second transition, which occurs at 11% v/v HFP, is between the self-associated form and an ordered monomeric form. The analysis of our experimental results demonstrates aggregate formation at 5–10% HFP. This may be relevant to the mechanism of channel formation by cecropins in membranes.

The cecropins are members of a class of antibacterial peptides that are widely distributed across the animal kingdom. First purified from the humoral immune response of the North American silk moth (Steiner *et al.*, 1981), cecropins have now been isolated from a variety of insect sources (Boman & Hultmark, 1987), as well as from the uppermost sector of the porcine small intenstine (Lee *et al.*, 1989). Insect cecropins are highly homologous, while the sequence homology between insect and mammalian cecropins is 33% (Lee *et al.*, 1989). Cecropins display strong antibacterial activity against both Gram-positive and Gram-negative bacteria. In addition, they induce membrane leakage in liposomes (Steiner *et al.*, 1988) and form voltage-dependent ion channels in planar bilayers (Christensen *et al.*, 1988). Cecropins embody many of the structural motifs implicated in membrane lysis, membrane protein insertion, and voltage-dependent conformational transitions.

Insect cecropins are well-characterized at the molecular level. The mechanism of cell killing has been proposed to occur via voltage-dependent ion-channel formation, or alternatively through membrane disintegration (Steiner *et al.*, 1988). The structural determinants of biological activity were studied using a large number of synthetic peptides with selective amino acid modifications (Andreu *et al.*, 1985). These studies emphasized the requirement for a flexible hinge region for antibacterial activity (Fink *et al.*, 1989) and led to a proposed helix–turn–helix structure that was confirmed by the NMR solution structure of cecropin A in 15% hexafluoro-2-propanol (HFP) (Holak *et al.*, 1988). Cecropins are highly unordered in solution and are assumed to be in a random coil conformation. When the polarity of water is reduced by the addition of HFP, the peptide folds into a 3-D structure characterized by two helical regions separated by a highly flexible turn. On the basis of the NMR results, the first helix was proposed to extend from residue 5 to residue 21, and the second from residue 25 to 37. The N-terminal helix is highly amphipatic and its positively charged residues are assumed to mediate binding to acidic lipids by sensing their local electrostatic potential. The highly conserved aromatic residue (Trp 2) flanking this helix at its N-terminus seems to anchor the peptide to the membrane. The hydrophobic C-terminal helix is proposed to strengthen membrane association by inserting vertically into the membrane hydrophobic core (Christensen *et al.*, 1988).

Recently, the solution structure of the mammalian cecropin P1 was solved in the presence of 30% HFP (Sipos *et al.*, 1992). Unlike insect cecropins, P1 apparently folds into a single helix that spans most of the peptide length. This structure is different from the structure of cecropin A despite the sequence homology between the two peptides and the evidence suggesting that the biological activity of cecropins is closely linked to the helix–turn–helix motif (Fink *et al.*, 1989).

This structural variability reflects the importance of the primary sequence in determining the conformation of short peptides. Position-specific side chain interactions such as the charged group effect (Marquese & Baldwin, 1987; Shoemaker *et al.*, 1987) and hydrophobic interactions between side chains (Lotan *et al.*, 1966) have been shown to play a major role in determining the structural stability of α helices in marginally stable peptides. The physical interactions involved in structural stability are of current interest due to the role secondary structures play in the initial steps of protein folding. Understanding the mechanisms by which unordered peptides assemble into a well-defined structure may give insight into the process of protein self-assembly. Small peptides such as the cecropins provide a tool for studying these mechanisms in simple and tractable model systems. The peptide conformations induced in response to changes in external parameters including ionic strength, temperature, and solvent polarity allow the elucidation of the forces that stabilize a particular conformation despite the large configurational space available.

† This work was supported by Grants GM22923 and RR01008 from the National Institutes of Health.

* Abstract published in *Advance ACS Abstracts,* October 15, 1993.

0006-2960/93/0432-11895$04.00/0

In this paper, we have studied the dynamics and aggregation state of a cecropin AD analogue in aqueous solution and in the presence of helix-promoting solvent. A cysteine was introduced into the hydrophobic C-terminus at position 33 and spin labeled using a methanethiosulfonate spin label (MTSSL).[1] The spin-labeling technique gives information on local structure and environment. This well-established approach was shown recently to be a powerful tool in investigating the dynamics of helix formation (Todd & Milhauser, 1991; Miick *et al.*, 1992), the structure of membrane proteins (Altenbach *et al.*, 1990; Shin *et al.*, 1993), and the binding of small peptides to lipid bilayers (Archer *et al.*, 1991). Much of this recent success can be attributed to the ability to introduce unique labeling sites by either site-directed mutagenesis or through peptide synthesis, allowing the selective investigation of specific domains or regions of secondary structure. We show here that cecropins can self-associate in the presence of 5–10% HFP. Our data suggest that the aggregate is stabilized by interpeptide interactions that might involve ion-pair formation. The self-association of the peptide is entropy driven; it is promoted by salt and destabilized by urea. The self-associated form of the peptide is significantly destabilized at pH below 5, and the peptide is completely monomeric at pH 3.5. Addition of higher percentages of HFP at neutral pH leads to the monomerization of the peptide in the folded state. These findings have important implications on the structure and mechanism of channel formation by cecropins and related peptides (Wade *et al.*, 1990).

MATERIALS AND METHODS

Materials. Cecropin A was obtained from Bachem (Torrance, CA). 1,1,1,3,3,3-Hexafluoro-2-propanol and 2,2,6,6-tetramethylpiperidine-1-oxyl (TEMPO) were obtained from Aldrich (Milwaukee, WI). Urea was obtained from United States Biochemicals (Cleveland, OH). (1-Oxyl-2,2,5,5,-tetramethylpyrrolin-3-yl)methyl methanethiosulfonate spin label was obtained from Reanal (Budapest, Hungary). Trifluoroacetic acid from Pierce (Rockford, IL) and acetonitrile from Fisher (Pittsburgh, PA) were HPLC grade. Reduced glutathione was obtained from Sigma (St. Louis, MO).

Peptide Synthesis, Labeling, and Purification. Cecropin AD (CAD) and Cys-33 CAD were synthesized at the Protein/Nucleic Acid Shared Facility of the Medical College of Wisconsin on a Milligen/Biosearch synthesizer, Model 9050. The instrument performs solid-phase peptide synthesis using FMOC-activated amino acid esters. Peptides were deprotected and removed from the resin with trifluoroacetic acid. The crude peptide (3–4 mg) was first purified by gel filtration on Bio-Gel P-2 (Bio-Rad, Richmond, CA) to remove low molecular weight contaminants, and then spin labeled by incubating with a 10-fold excess of the methanethiosulfonate spin label for 4 h at room temperature. The labeled peptide was then purified by reverse-phase HPLC on an 8 × 100 mm Waters Delta-Pack C18 semipreparative column with 15-μm particles and 100-Å pore size. Comparison of the elution profiles of cecropin A, cecropin AD, and MTSSL–Cys-33 CAD show that both CAD and its labeled analogue are more hydrophobic than cecropin A as reported previously (Fink *et al.*, 1988). MTSSL–Cys-33 CAD was slightly more hydrophobic than the native CAD. The sequences of the purified peptides were verified by amino acid analysis on a Beckman 6300 amino acid analyzer. The molecular weight of purified CAD was confirmed by mass spectrometry performed on a Kratos fast atom bombardment (FAB) mass spectrometer at the Protein/Nucleic Acid Shared Facility at the Medical College of Wisconsin. Mass spectral analysis of the purified spin-labeled peptide was performed by plasma desorption ionization using time-of-flight detection on a ABI Bio-Ion 20 mass spectrometer (Multiple Peptide Systems, San Diego, CA). Reduced glutathione was used as received. Excess glutathione was labeled with MTSSL and purified by reverse-phase HPLC.

Electron Spin Resonance (ESR). A Varian E-109 spectrometer (Varian Assoc., Palo Alto, CA) fitted with a two-loop one-gap resonator (Hyde & Froncisz, 1989) was used for CW ESR measurements. Samples of 5 μL were loaded in 0.84 mm o.d. capillaries and sealed on both ends. The magnetic field was stabilized with a Varian field-frequency lock. Data acquisition was controlled by a PC interfaced to the spectrometer utilizing the VIKING software package (C. C. Felix, National Biomedical ESR Center, Milwaukee, WI).

Motionally narrowed spectra used for the determination of line-width parameters and the rotational correlation times were taken with modulation amplitude in the range of 0.3–0.4 G. For motionally restricted or spin–spin broadened spectra, a 1.6–2.5 G modulation amplitude was used. All spectra were acquired using 1 mW of microwave power.

The rotational correlation time and line-width parameters B and C of fast-tumbling spin label were obtained according to Todd and Millhauser (1991). No correction was made to account for inhomogeneous broadening since it introduces an error of less than 10%. For spectra characterized by slow tumbling, such as those shown in Figure 6, the rotational correlation time was calculated using the program developed by Freed and co-workers (Schneider & Freed, 1989) and running on a 486/50 MHz PC.

The spin-label concentration for the labeled peptide was determined by double integration of the ESR spectrum followed by comparison with a standard aqueous TEMPO solution. The peptide concentration was determined from the optical absorbance at 280 nm using an extinction coefficient of 5600/M cm. At this wavelength only the tryptophane side chain absorbs while at 250 nm the spin-label absorbance dominates (Altenbach and Hubbell, 1988). From the absorbance ratio, the 1:1 peptide to spin-label ratio was verified.

RESULTS

Dynamics and Aggregation State of MTSSL–Cys-33 CAD in Aqueous Solution. The room-temperature ESR spectrum of MTTSL–Cys-33 CAD in aqueous solution at different ionic strengths is shown in Figure 1. In the absence of spin exchange, the ESR line widths reflect dynamic effects induced by molecular reorientation of the spin label around its point of attachment as well as global reorientation of the peptide. The sharp lines in Figure 1 indicate rapid isotropic motion of the spin label, with a 0.48-ns correlation time. No change in the spectral line widths is detected upon the addition of 250 mM salt. The ESR spectra in water and in 250 mM NaCl are indicative of a random coil structure in solution, consistent with previously reported CD data (Andreu *et al.*, 1985). The random coil structure is further confirmed in Figure 2. where the parameters B and C are shown for a temperature range of 1–55 °C. In the fast motional regime the ratio B/C is independent of the correlation time and reflects mainly

[1] The amino acid sequence of Cys-33 CAD is K-W-K-L-F-K-K-I-E-K-V-G-Q-R-V-R-D-A-V-I-S-A-G-P-A-V-A-T-V-A-Q-A-C-A-L-A-K-NH_2.

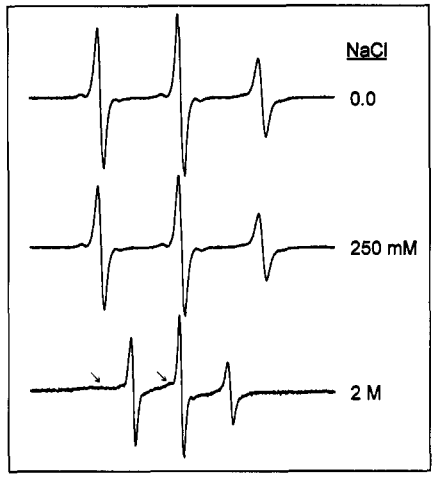

FIGURE 1: ESR spectra of spin-labeled CAD in the monomer conformation at different ionic strengths. The aqueous solution contained 20 mM Hepes at pH = 7. The arrows indicate the less mobile species. The 2 M NaCl spectrum was taken with 100 G scan width; while the other two spectra have a 60 G scan width.

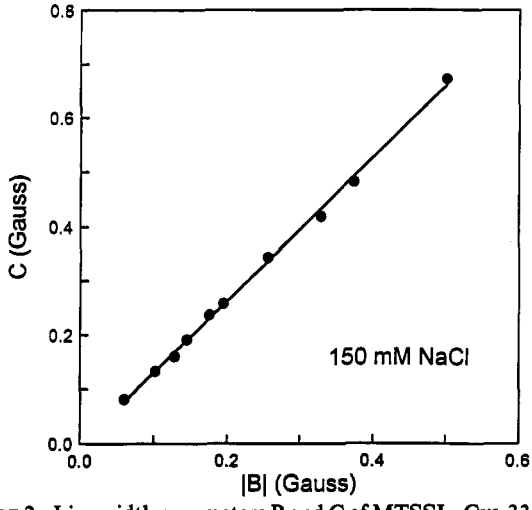

FIGURE 2: Line width parameters B and C of MTSSL–Cys-33 CAD in 150 mM NaCl as a function of temperature. The slope of the linear regression fit is 1.3.

motional anisotropy (Goldman *et al.*, 1972). A constant slope such as that in Figure 2 indicates a constant motional anisotropy across the whole temperature range. Also shown in Figure 1 is the ESR spectrum of MTSSL–Cys-33 CAD in the presence of 2 M NaCl. This spectrum shows evidence of two spin populations with different motional mobilities. One component is characteristic of rapid reorientation of the spin label, while the other minor component indicates either slower motion, spin–spin interaction, or a combination of both.

The possibility of concentration-dependent aggregation can be probed by investigating the dependence of the signal amplitude of the $m_I = 0$ resonance (center line) on peptide concentration. Aggregation that produces electron spin–spin interactions will lead to a nonlinear dependence of the spectral amplitude on concentration. Figure 3 shows a completely linear increase in the intensity of the $m_I = 0$ resonance as the peptide concentration increases, both in the presence and absence of 150 mM NaCl. Furthermore, no changes in the rotational correlation time were detected as a function of peptide concentration (data not shown). These results clearly indicate that the peptide remains monomeric across the entire range of concentrations examined (10–200 μM), both in water and in 150 mM NaCl. In 2 M NaCl spin–spin interaction is detected at concentrations >40 μM, reflecting the existence of an aggregate with a conformation that brings spin-labeled sites into close proximity.

Structural Transitions in the Presence of HFP. The cecropins have been shown to adopt a mainly helical structure in the presence of HFP. The 2D NMR structure, solved in 15% HFP, shows the existence of a helix–turn–helix motif. CD spectroscopy of cecropin A shows that adoption of helical secondary structure starts at about 5%, reaches a maximum at 10%, and then levels off with a small decrease for higher percentages of HFP (Andreu *et al.*, 1985). Figure 4 shows ESR spectra of MTSSL–Cys-33 CAD in the presence of different percent concentrations of HFP. Between 5% and 10% (v/v), the spectrum drops in amplitude and shows two spin-label populations with different rotational mobility. The broad component indicates the existence of a species with slower rotational correlation time and/or an aggregate in which the lines are broadened by spin–spin interactions, while the component with three sharp lines represents a very small fraction of unfolded and/or monomeric peptide. The large decrease in signal amplitude is due to line broadening, since the doubly integrated signal intensity remained constant. At a volume percentage of HFP higher than 13%, the broad component virtually disappears, leaving a single species with a correlation time significantly slower than the unordered peptide, most likely due to monomeric peptide in a folded conformation. Control experiments were performed by titration of MTSSL-labeled glutathione with the same concentrations of HFP. No major changes in signal amplitude or line shapes were detected for this unordered peptide (data not shown). Only minor effects due to changes in viscosity were observed.

This result indicates a conformational transition of spin-labeled cecropin AD as the volume percentage of HFP is increased. The broadened line shape observed at 5–10% HFP (Figure 4) could arise either from motional restriction of the spin label due to peptide folding or from line width increase arising from peptide aggregation induced spin–spin interaction or a combination of both. In order to analyze the line shape of the aggregate spectrum, the two contributions to the line width must be separated.

Dynamics and Aggregation State of the Peptide in HFP. The marked decrease in signal intensity observed at 5–10% HFP suggests peptide aggregation. If the aggregate contains more than one spin-labeled peptide, the spin labels may interact by Heisenberg exchange and/or electron dipole–dipole interactions, which shorten the effective relaxation rates and lead to increased line width and decreased intensity. Therefore, we compared the signal amplitude of a constant amount of MTSSL–Cys-33 CAD in the presence of increasing amounts of nonlabeled native cecropin AD (having threonine at position 33). Figure 5 shows the dependence of the signal amplitude of the $m_I = 0$ resonance line on N, the mole ratio of unlabeled CAD to spin-labeled MTSSL–Cys-33 CAD. The signal amplitude increases by as much as 3-fold as increasing amounts of unlabeled peptide are added, diluting the number of spins in each putative aggregate. A similar increase in signal amplitude results upon addition of excess cecropin A (data not shown). This result indicates the presence of an aggregated peptide species in a conformation that brings the spin-labeled sites, located in the C-terminal domain, into close proximity.

The stability of the peptide aggregate can be probed by investigating its dependence on total peptide concentration. As found in Figure 3, the signal amplitude increases linearly with peptide concentrations in the presence of 10% HFP,

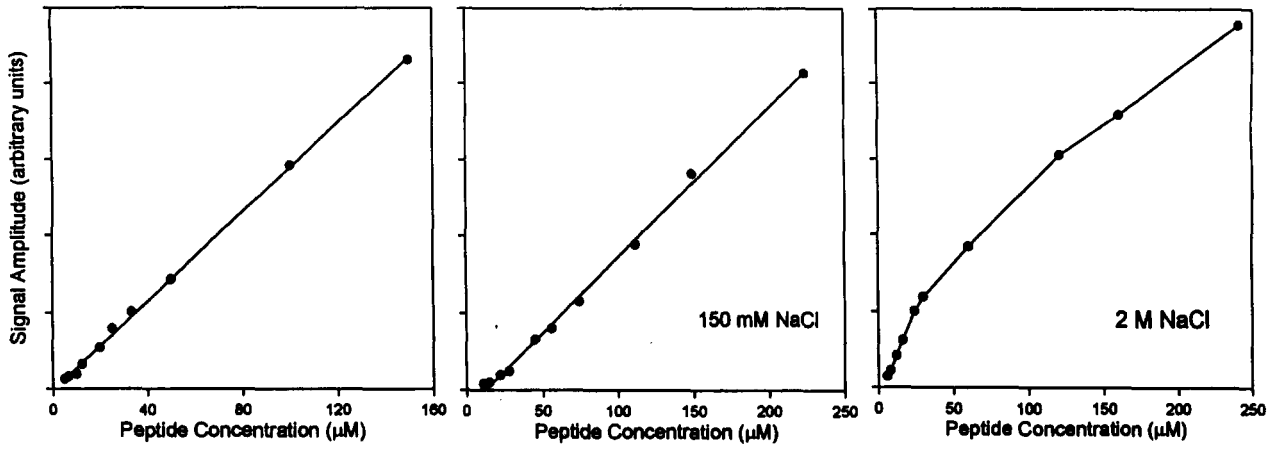

FIGURE 3: Signal intensity of the $m_I = 0$ resonance of MTSSL–Cys-33 CAD spectra as a function of peptide concentration at different ionic strengths. The aqueous solution contained 20 mM Hepes, pH = 7.

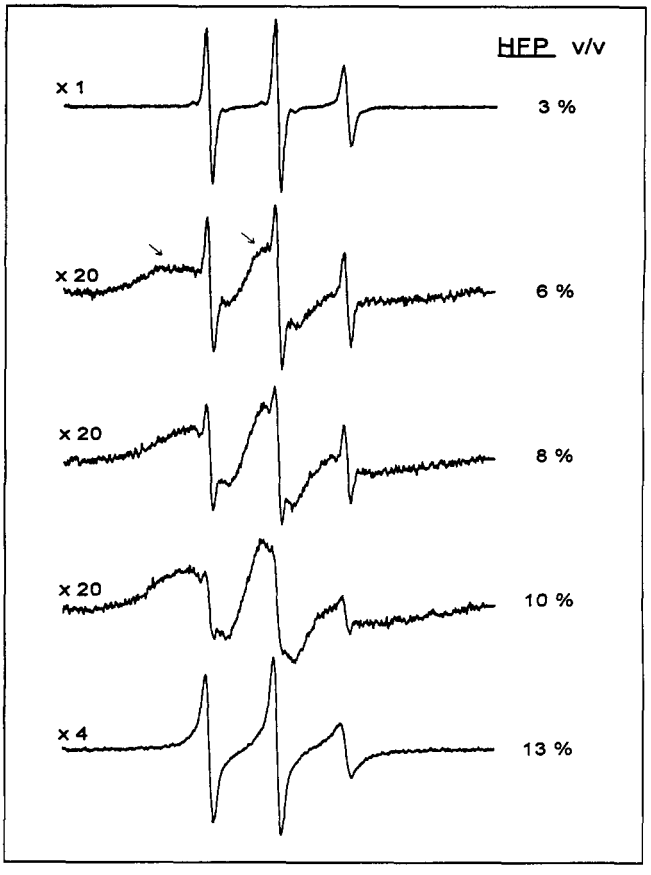

FIGURE 4: ESR spectra of 150 μM MTSSL–Cys-33 CAD in the presence of different HFP concentrations. The arrows indicate the motionally restricted component of the spectrum. The aqueous solution contained 20 mM Hepes, pH = 7.

indicating a constant spin–spin interaction contribution to the line width. Therefore, in the concentration range used, decreasing the amount of peptide does not decrease the stability of the aggregate, i.e., changes in the aggregate–monomer equilibrium are not observed as a function of peptide concentration. In addition, higher peptide concentration does not change the number of monomers per aggregate. These results indicate the formation of a well-defined, highly stable aggregate that does not readily dissociate in 10% HFP. Similar formation of a stable peptide aggregate has been previously reported (Ho & Degrado, 1985).

Motional restriction also plays a role in producing the broadened line shape observed at intermediate HFP concentrations. If there is only one spin-labeled peptide in the aggregate, then one can extract from the spectrum the motional parameters. Figure 6 shows ESR spectra of MTSSL–Cys-33 CAD in the presence of a 10-fold excess native CAD at different volume percentages of HFP. From the spectra of these spin-diluted samples, where spin–spin interactions have been largely eliminated, it is apparent that at HFP concentrations higher than 6% the motion of the spin label is considerably restricted. Therefore, the change in mobility of the spin label in going from 3% to 10% HFP is due to motional restriction of the spin label in the aggregate. The rotational correlation time at 9% HFP is estimated to be 3 ns. In going from 10% to 13% HFP, the ESR spectrum reflects an increase in rotational freedom. At 13% HFP, the rotational correlation time is $\simeq$1 ns. This is consistent with monomerization of the peptide at higher percentages of HFP. Rotational motion of the spin label at 13% HFP is decreased relative to that observed at 0–3% HFP, reflecting the difference in folded and random coil conformations, respectively.

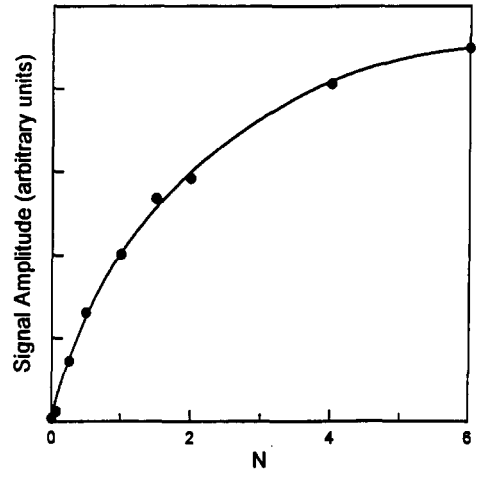

FIGURE 5: Signal amplitude of the $m_I = 0$ resonance of the same amount of MTSSL–Cys-33 CAD as a function of the mole ratio between native CAD and labeled CAD. Each sample contained 80 μM MTSSL–CAD, 10% HFP, 20 mM Hepes, pH = 7.

Physical Forces Involved in Stabilizing Peptide Aggregates. In order to determine the physical interactions involved in promoting these structural transitions, we studied the dependence of aggregate formation on ionic strength, pH, temperature, and urea concentration. Salts increase the hydrophobic interaction through their effects on the structure of water, while they shield interacting charges and weaken

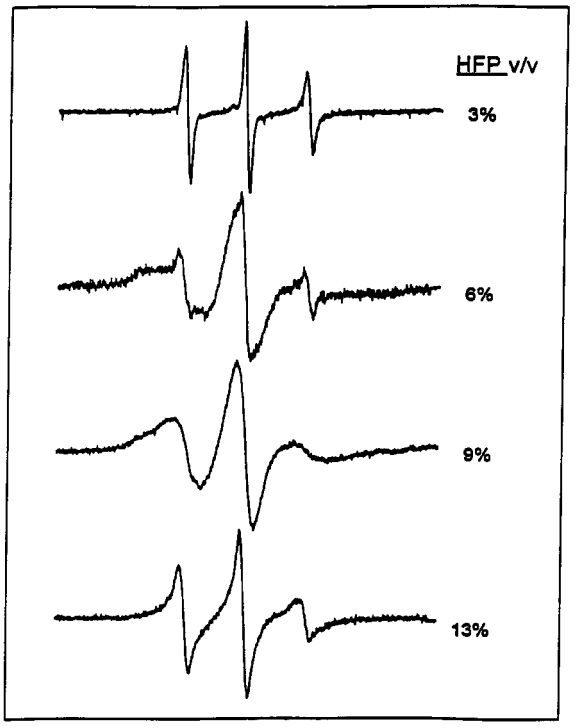

FIGURE 6: ESR spectra of spin-labeled CAD in the presence of a 10-fold excess CAD at different concentrations of HFP. Each sample contained 40 μM MTSSL–Cys-33 CAD, 400 μM CAD, 20 mM Hepes, pH = 7.

electrostatic interactions. If aggregation involves the formation of salt bridges, then it will be destabilized in high ionic strength solution. An opposite effect will result if interpeptide interaction is hydrophobic or is modulated by electrostatic repulsion between lysines side chains. The rationale for studying the effect of NaCl on peptide aggregation is to determine the net effect of these forces. Figure 7 shows the change in aggregate formation as the concentration of NaCl increases. The experiment was conducted at 5% HFP, where the peptide exists in a monomer–aggregate equilibrium. The equilibrium is shifted toward aggregate formation as the ionic strength increases. At 10% HFP, high-salt concentration (0.75 M) leads to a slight decrease in aggregate stability (data not shown). More important is the fact that aggregate formation in the 5–10% HFP range becomes nearly flat.

If self-association is driven by hydrophobic interactions or ion-pair formation, then in a limited temperature range, increased temperature will stabilize the aggregate (Creighton, 1984). Figure 8 shows the change in the ESR spectrum of MTSSL–Cys-33 CAD as a function of temperature in 5% HFP. The broad component characteristic of the aggregate disappears at low temperature and is enhanced at higher temperatures, pointing to an entropy-driven self-association.

In order to distinguish between stabilizing interactions, we compared aggregate formation at different pH. Different states of side-chain ionization should alter the stabilizing effect of ion-pair formation without significantly affecting the contribution of hydrophobic interactions. Figure 9 illustrates the effect of pH titration on aggregation stability. The increased spectral intensity as well as the narrower line shape at acidic pH indicates a decrease in the extent of peptide self-association. Our data suggests that the pK_a of the titrated group is between 4 and 5. Remarkably, this value corresponds to the pK_a of glutamate (Glu-9) that was recently suggested to mediate cecropin dimer formation via ion pairing to Arg-16 (Durell *et al.*, 1992).

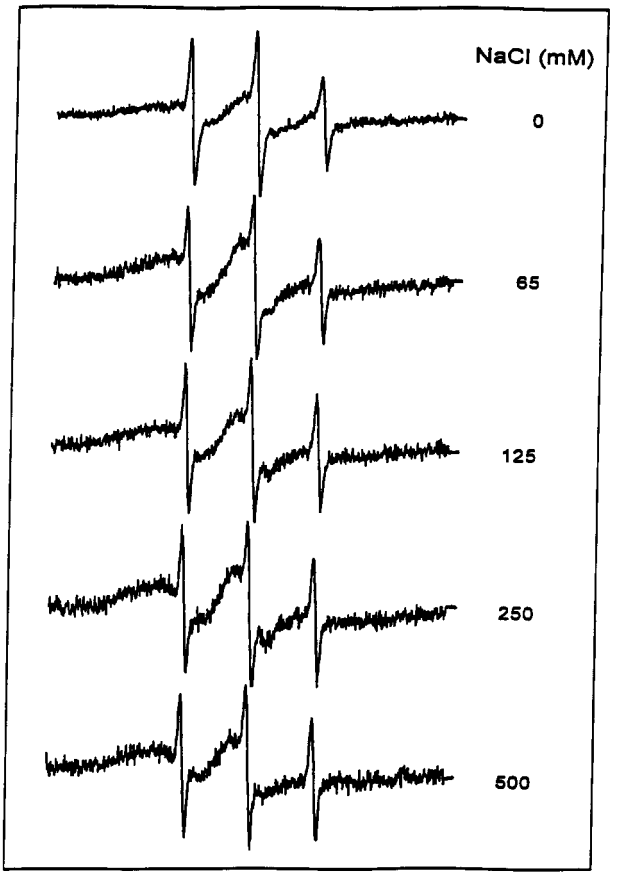

FIGURE 7: Dependence of peptide self-association on ionic strength at 5% v/v HFP. Each sample contained 80 μM MTSSL–Cys-33 CAD, 20 mM Hepes, pH = 7. The temperature was maintained at 293 K.

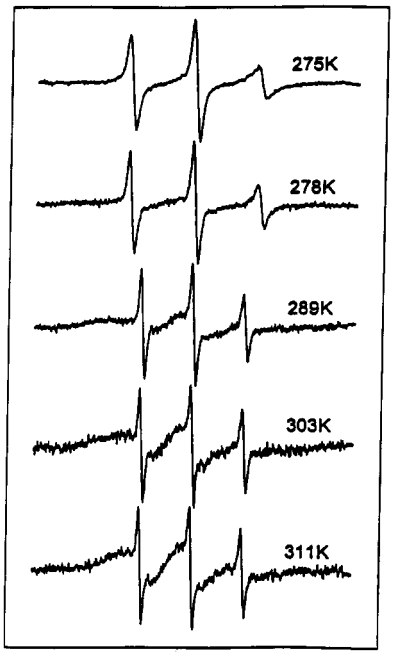

FIGURE 8: Effect of temperature on peptide structure at 5% v/v HFP.

We also examined the effect of urea on peptide aggregation. Urea is known to increase the solubility of nonpolar side chains while maintaining the hydrogen-bonding potential of the aqueous solvent. In globular proteins, urea increases the accessible surface area, diminishing the hydrophobic effect by one-third (Creighton, 1984). Figure 10 shows the effect

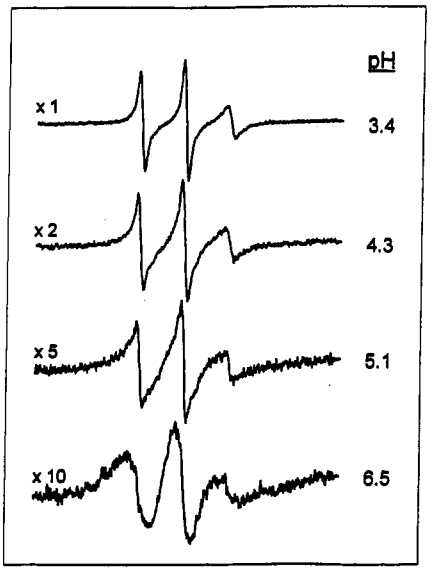

FIGURE 9: Dependence of peptide self-association on side-chain ionization. Each sample contained 50 μM MTSSL–Cys-33 CAD, 9% v/v HFP, 50 mM acetate. The pH was adjusted with a 50 mM solution of acetic acid.

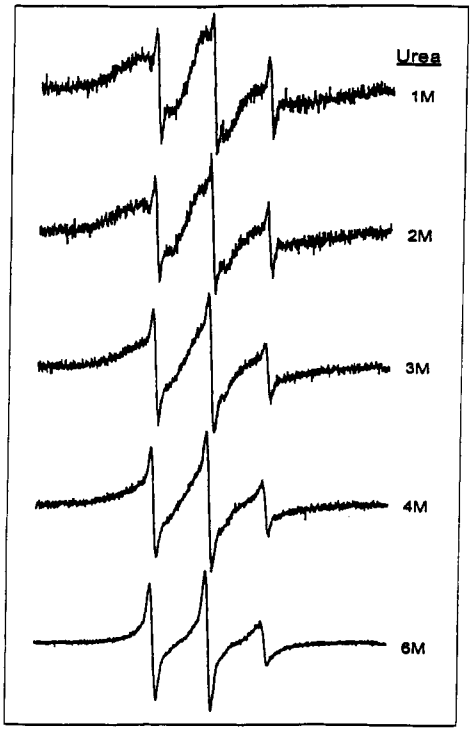

FIGURE 10: Effect of urea on the structure of the self-associated peptide. Each sample contained 70 μM MTSSL–Cys-33 CAD, 9% v/v HFP, 20 mM Hepes, pH = 6.7.

of urea on the peptide structure in the presence of 10% HFP. The aggregate is significantly destabilized in the presence of urea. The extent of aggregation, monitored by the broad shoulder of the low field line, decreases as the urea concentration increases. The effect of urea on the spin-diluted aggregate (containing 10-fold excess unlabeled CAD) is illustrated in Figure 11. This spectrum, taken in 7 M urea, at 9% HFP, is qualitatively similar to that observed at 13% HFP in the absence of urea (see Figure 4). It is difficult to assess the extent of secondary structure destabilization by urea from the line shape due to the effects of viscosity changes in the presence of high urea concentrations. It has been shown previously that although urea leads to disruption of helix-

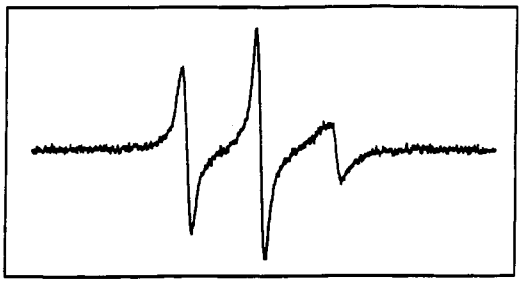

FIGURE 11: Effect of 7 M urea on the line shape of the spin-diluted aggregate. Each sample contained 40 μM MTSSL–Cys-33 CAD, 400 μM CAD, 9% v/v HFP, 20 mM Hepes, pH = 6.7.

helix contact in coiled coils, the helix monomers can retain a significant fractional helicity (Lau *et al.*, 1984). The increased mobility of the spin label in the spin-diluted aggregate and the disappearance of spin–spin interactions are consistent with peptide monomerization in the presence of urea.

DISCUSSION

The cecropins are characterized by a structural motif that includes a hydrophobic amidated C terminus and a hydrophilic basic amino terminal region connected by a highly flexible turn. Both the N- and C-terminal regions adopt a mainly helical conformation in the presence of HFP (Andreu *et al.*, 1985; Holak *et al.*, 1988). It was shown previously that the helical and basic character of the N-terminal domain is crucial for antibacterial activity while the C terminus has a less important role although its hydrophobocity enhances activity (Fink *et al.*, 1989). Cecropin AD, constructed from the N-terminal sequence of cecropin A and the more hydrophobic C terminus of cecropin D, has enhanced channel activity and is a more potent antibiotic than either of the naturally occurring peptides (Fink *et al.*, 1988).

The aggregation state of cecropin AD in solution is determined by two opposing interactions: the tendency of its hydrophobic C terminus to aggregate and the electrostatic repulsion between the charged residues of the N terminus. Two observations led previous investigators to consider the possibility of cecropin self-association. The first was the high lethal concentration needed in antibacterial assays (Steiner *et al.*, 1988). The second was the weak dependence of cecropin-induced conductance in planar bilayers on concentration (Christensen *et al.*, 1988). It is also desirable to sequester hydrophobic residues in the C-terminal domain from aqueous solvent, which could be accomplished by interpeptide association. Our data suggest that the peptide is monomeric in low ionic strength aqueous solution at pH 7. Addition of low concentrations of salt or changes in temperature does not alter its state or conformation significantly. In general, water acts as a denaturant of short peptides; its high polarity and basicity destabilizes intramolecular hydrogen bonds, allowing it to compete effectively for peptide hydrogen-bond donors and acceptors (Llinas & Klein, 1974), apparently preserving the random coil structure of cecropin AD.

Effect of Solvent Polarity on Peptide Structure. Upon addition of 5–10% (v/v) HFP, a monomer aggregate equilibrium is observed. That the peptide is induced to aggregate is evident from the presence of spin–spin interactions and the increase in motional restriction. CD spectroscopy shows that this is the same HFP range that induces maximum helicity (Andreu *et al.*, 1985). Our data shows that for higher percentages of HFP the peptide reverts to a monomeric, ordered state. This is also in agreement with previous studies

using NMR and CD (Holak *et al.*, 1988). Thus, the peptide switches between two ordered forms by passing from a folded aggregate stabilized by interpeptide interactions to a folded monomeric state (most probably the proposed helix–turn–helix) stabilized by intramolecular interactions. It is likely that aggregation and helix formation are concomitant events due to the energy cost of transferring unsatisfied hydrogen-bond donors or acceptors from an aqueous environment. The transition between the two is very abrupt, occurring over a 1–2% change in HFP, as in the initial transition from the unordered to the aggregated form, indicative of a cooperative system. This structural polymorphism has been detected previously for the peptide maganin in a trifluoroethanol–water mixture (Marion *et al.*, 1988). These structural transitions involve two important aspects of protein folding: helix formation and helix–helix interaction.

The effect of fluorinated alcohols on peptide conformation has been attributed to their weak hydrogen-bond-acceptor properties that helps promote hydrogen bonding by the amide nitrogen (Sonnichsen *et al.*, 1992). The hydrogen bonds most important for helix formation are those between amide nitrogen and carbonyl oxygen; therefore, these solvents induce helix formation in regions with helical propensiy. In addition, these solvents lower the dielectric constant of water; however, it is assumed that they do not significantly enhance charged-group interactions (Nelson & Kallenbach, 1986). At high concentrations, fluorinated alcohol can lead to the disruption of protein quaternary structure by decreasing hydrophobic interactions. Trifluoroethanol was shown to disrupt helix–helix contact in coiled coils, producing single-stranded helical monomers (Lau *et al.*, 1984).

The presence of HFP apparently promotes helix formation in both the N- and C-terminal regions of cecropin AD (Holak *et al.*, 1988). Our data suggest that, between 5–10% v/v HFP, peptide folding results from a balance of electrostatic, hydrophobic, and hydrogen-bonding energies with unfavorable conformational entropy. The stability of both helical regions seems to depend on the peptide aggregation. However, many questions must be resolved to understand the contribution of the various factors to self-association as well as folding of the peptide. The pH and temperature dependencies of the self-association process suggest that it is promoted by interpeptide contacts that might involve ion-pair formation and hydrophobic interactions. We cannot distinguish whether it is an intra- or an intermolecular ion pair, especially if helix formation and peptide aggregation are concerted processes at 10% HFP. However, there is no positively-charged side chain a suitable distance (i.e., four residues) from Glu-9, which may suggest that the ion pair is intermolecular and mediates antiparallel dimer formation (Durrell *et al.*, 1992). As the polarity of the medium is further reduced by the addition of HFP, the water activity is lowered to an extent where contact between solvent and side chains lead to a shift in the aggregate–monomer equilibrium toward the latter. This illustrates the importance of solvent–peptide interactions in determining the induced conformation of the peptide.

Implications for Channel Formation. The generally accepted mechanism for the voltage-dependent formation of channels by short peptides is the insertion of helices followed by aggregation into oligomeric structures (Lear *et al.*, 1988). In the detailed model offered by Durell *et al.*, the C-terminal helices of cecropin dimers aggregate in a manner that allows a variety of hydrophobic contacts and hydrogen bonds to be made, thus stabilizing the formation of the channel. Our results indicate the formation of peptide aggregates in 10% HFP promoted mainly by a combination of hydrophobic and electrostatic interactions. It is generally assumed that fluorinated alcohols in water mimic low dielectric media such as the membrane core or hydrophobic-protein interior. However, the correspondence between the state of the peptide in the isotropic solvent and that adopted in the highly directional membrane environment is unclear.

Close packing, hydrogen bonding, and salt-bridge formation have been proposed to drive the association of local regions in transmembrane helices (Popot & Engelman, 1990). From this perspective, the aggregate observed in 10% HFP becomes an important indication for the possibility of helix–helix packing that is more favorable than lipid packing against the irregular surfaces of helices. The stability of the self-associated form of the peptide indicates the possible formation of van der Waals contacts and hydrogen bonds that require a high degree of complementarity between the surfaces involved.

The energetics of aggregate formation in water is different than in the bilayer. In isotropic solvents, peptide self-association leads to the loss of translational and rotational entropy, which has been estimated for the case of dimer formation to be 15 kcal/mol (Janin & Chothia, 1990). Reduction in accessible surface area occurring upon peptide association provides the major free energy contribution in naturally occurring helical bundles (Chothia & Finkelstein, 1990). Energy balance requires that the gain in hydrophobic free energy that results from the reduction in nonpolar residues in contact with water compenstate for this loss. The free energy of hydrophobic interaction gained by burying 1 Å^2 of surface area has been estimated to be 25 cal/mol (Chothia, 1974). For oligomeric protein the accessible surface area that becomes buried when monomers come together varies between 1000 and 5500 Å^2, the lower limit values occurring when the structure of the associated and isolated monomers are very similar (Chothia & Janin, 1975). In membranes, the unfavorable entropic term is smaller since a surface-bound peptide has already lost one translational and two rotational degrees of freedom in the initial binding step. Thus for a pair of helices, a single hydrogen bond or salt bridge can compensate for the entropic loss (Popot & Engelman, 1990).

CONCLUSION

We have used a spin-labeling technique to study the dynamics and aggregation of cecropin AD in aqueous solution and in the presence of a helix-promoting solvent. We have shown that cecropin AD can self-associate in the presence of 5–10% HFP and that the aggregation process is promoted largely by hydrophobic interactions and ion-pair formation. A similar aggregate may exist in the low dielectric environment of the lipid bilayer and can be involved in channel formation. Further application of site directed spin labeling should allow systematic investigation of this question.

ACKNOWLEDGMENT

The authors thank Dr. A. L. Haas, Department of Biochemistry, Medical College of Wisconsin, for helpful suggestions and critical reading of the manuscript.

REFERENCES

Altenbach, C., & Hubbell, W. (1988) *Proteins 3*, 230–242.

Altenbach, C., Marti, T., Khorana, H. G., & Hubbell, W. L. (1990) *Science 248*, 1088–1092.

Andreu, D., Merrifield, R. B., Steiner, H., & Boman, H. G. (1985) *Biochemistry 24*, 1683–1688.

Archer, S. J., Ellena, J. F., Cafiso, D. S. (1991) *Biophys. J. 60*, 389–398.
Boman, H. G., & Hultmark, D. (1987) *Ann. Rev. Microbiol. 41*, 103–126.
Chothia, C. (1974) *Nature 248*, 338–339.
Chothia, C., & Janin, J. (1975) *Nature 256*, 705–708.
Chothia, C., & Finkelstein, A. V. (1990) *Annu. Rev. Biochem. 53*, 1007–1039.
Christensen, B., Fink, J., Merrifield, R. B., & Mauzerall, D. (1988) *Proc. Natl. Acad. Sci. U.S.A 85*, 5072–5076.
Creighton, T. E. (1984) in *Proteins: Structures and Molecular Properties*, Freeman, New York.
Durell, S. R., Ragohunathan, G., & Guy, H. R. (1992) *Biophys. J. 63*, 1623–1631.
Fink, J., Merrifield, R. B., & Boman, H. G. (1988) *J. Biol. Chem. 264*, 6260–6267.
Fink, J., Boman, A., Boman, H. G., & Merrifield, R. B. (1989) *Int. J. Pept. Protein Res. 33*, 412–421.
Goldman, S. A., Bruno, G. V., Polnaszek, C. F., & Freed, J. H. (1972) *J. Chem. Phys. 56*, 716–735.
Ho, S. P., & Degrado, W. F. (1987) *J. Am. Chem. Soc. 109*, 6751–6758.
Holak, T. A., Engström, A, Kraulis, P. J., Lindeberg, G., Bennich, H., Jones, T. A., Groenenborg, A. M., & Clore, G. M. (1988) *Biochemistry 27*, 7260–7269.
Hyde, J. S., & Froncisz, W. (1989) in *Advanced EPR Applications in Biology and Biochemistry* (Hoff, A. J., Ed.) Chapter 7, Elsevier, Amsterdam.
Janin, J., & Chothia, C. (1990) *J. Biol. Chem. 267*, 16027–16030.
Lau, S. Y. M., and Taneja, A. K. S., Hodges, R. S. (1984) *J. Biol. Chem. 259*, 13253–13261.
Lear, J. D., Wasserman, Z. R., & DeGrado, W. F. (1988) *Science 240*, 1177–1181.
Lee, J. Y., Boman, A., Chunxin, S., Andersson, M., Jörnvall, H., Mutt, V., & Boman, H. G. (1989) *Proc. Natl. Acad. Sci. U.S.A. 86*, 9159–9162.
Llinas, M., & Klein, M. P. (1974) *J. Am. Chem. Soc. 97*, 473–4737.
Lotan, N., Yaron, A., & Berger, A. (1966) *Biopolymers 4*, 365–368.
Marion, D., Zasloff, M., & Bax, A. D. (1988) *FEBS Lett. 227*, 21–26.
Marquese, S., & Baldwin, R. L. (1987) *Proc. Natl. Acad. Sci. U.S.A. 84*, 8898–8902.
Miick, S. M., Martinez, G. V., Fiori, W. R., Todd, A. P., & Millhauser, G. L. (1992) *Nature 359*, 653–655.
Nelson, J. W., & Kallenbach, N. R. (1986) *Proteins 1*, 211–217.
Popot, J. L., & Engelman, D. M. (1990) *Biochemistry 29*, 4031–4037.
Schneider, D. J., Freed, J. H. (1989) in *Biological Magnetic Resonance* (Berliner, L. J., and Reuben, J., Eds.) Chapter 1, Plenum, New York.
Shin, Y.-K., Levinthal, C., Levinthal, F., Hubbell, W. L. (1993) *Science 259*, 960–963.
Shoemaker, K. R., Kim, P. S., York, E. J., Stewart, J. M., & Baldwin, R. L. (1987) *Nature 326*, 563–567.
Sipos, D., Anderson, M., & Ehrenberg, A. (1992) *Eur. J. Biochem. 209*, 163–169.
Sönnichsen, F. D., Van Eyk, J. E., Hodges, R. S., & Sykes, B. D. (1992) *Biochemistry 31*, 8790–8798.
Steiner, H., Hultmark, D., Engström, A, Bennich, H., & Boman, H. G. (1981) *Nature 292*, 246–248.
Steiner, H., Andreu, D., & Merrifield, R. B. (1988) *Biochim. Biophys. Acta 939*, 260–266.
Todd, A. P., & Millhauser, G. L. (1991) *Biochemistry 30*, 5515–5523.
Wade, D., Boman, A., Wahlin, B., Drain, C. M., Andreu, D., Boman, H. G., & Merrifield, R. B. (1990) *Proc. Natl. Acad. Sci. U.S.A. 87*, 4761–4765.